Kinetic and Mechanistic Analysis of Nonenzymatic, Template-Directed Oligoribonucleotide Ligation

Rajat Rohatgi, David P. Bartel,[†] and Jack W. Szostak*

Contribution from the Department of Molecular Biology, Massachusetts General Hospital, Boston, Massachusetts 02114

Received November 3, 1995[⊗]

Abstract: The role of divalent cations in the mechanism of pyrophosphate-activated, template-directed oligoribonucleotide ligation has been investigated. The dependence of the reaction rate on Mg^{2+} concentration suggests a kinetic scheme in which a Mg^{2+} ion must bind before ligation can proceed. Mn^{2+}, Ca^{2+}, Sr^{2+}, and Ba^{2+} can also catalyze the reaction. Although Pb^{2+} and Zn^{2+} do not catalyze the reaction in the absence of other divalent ions, they significantly modulate the reaction rate when added in the presence of Mg^{2+}, with Pb^{2+} stimulating the reaction (up to 65-fold) and Zn^{2+} inhibiting the reaction. The logarithm of the ligation rate increases linearly, with slope of 0.95, as a function of pH, indicating that the reaction involves a single critical deprotonation step. The ligation rates observed with the different divalent metal ion catalysts ($Mn^{2+} > Mg^{2+} > Ca^{2+} > Sr^{2+} = Ba^{2+}$) vary inversely with the pK_a values of their bound water molecules. The pH profile and these relative ligation rates suggest a mechanism in which a metal-bound hydroxide ion located near the ligation junction promotes catalysis, most likely by deprotonation of the hydroxyl nucleophile. The effects of changing either the leaving group or the attacking hydroxyl, together with the large $\Delta S^{\ddagger}$ value for oligonucleotide ligation (about −20 eu), are consistent with an associative transition state.

Nonenzymatic, template-directed RNA polymerization reactions have been extensively studied over the past 30 years[1−3] because they model the type of reaction thought to have been important in the origin of life.[3] Much of this work has focused on the template-directed polymerization of mononucleotides activated with imidazole and carbodiimide derivatives.[2] A nonenzymatic replication scheme that has been less thoroughly investigated involves the template-directed ligation of short $3'−5'$-linked oligomers rather than monomers. We recently described the detection of a nonenzymatic ligation of two oligoribonucleotides aligned on a template RNA in which the 3'-hydroxyl of one oligonucleotide attacks the 5'-triphosphate of the other oligonucleotide, displacing pyrophosphate with the concomitant formation of a $3'−5'$ phosphodiester bond (Figure 1).[4] Despite its slow rate ($t_{1/2} \approx 15−30$ years at pH 7.4 and 100 mM Mg^{2+}), this oligonucleotide ligation reaction has several interesting properties. First, this reaction serves as a nonenzymatic correlate for the study of various enzyme-catalyzed reactions that involve the synthesis of phosphate esters. Nucleophilic attack on a phosphomonoester−monoanhydride (the α-phosphate of a 5'-triphosphate) is analogous to the chemical transformation catalyzed by DNA and RNA polymerases, polynucleotide ligases, and certain RNA ligase ribozymes.[4] Further study of the nonenzymatic reaction may lead to useful insights into the mechanisms by which both protein and RNA enzymes achieve their remarkable rate accelerations. Second, the reaction has a high propensity to form $3'−5'$ rather than $2'−5'$ phosphodiester bonds. Attack by the 3'-hydroxyl to yield the $3'−5'$ phosphodiester bond typical of informational nucleic
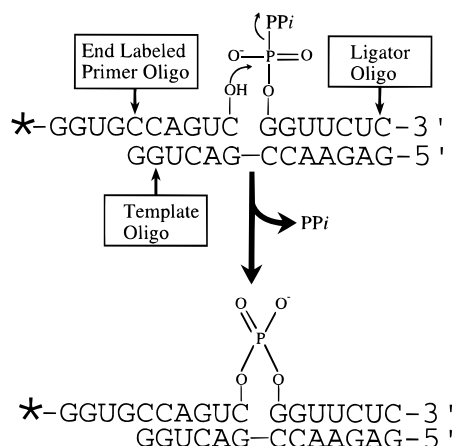

Figure 1. Schematic of the ligation reaction. Primer and ligator RNAs are aligned by contiguous Watson−Crick base-pairing with a template RNA. The 3'-hydroxyl of the primer attacks the α-phosphate of the 5'-triphosphate of the ligator to form a phosphodiester bond, with the release of pyrophosphate (PP*i*). The asterisk indicates a ^{32}P-labeled phosphate.

acids is 60 times faster than attack by the 2'-hydroxyl to yield a $2'−5'$ linkage.[5] Third, activation of the α-phosphate by pyrophosphate not only is ubiquitous in modern-day biological systems but also is thought to be more plausible in a prebiotic environment than is activation by imidazole or carbodiimide.[3]

Here we report the kinetic and mechanistic characterization of the pyrophosphate-activated, template-directed oligoribonucleotide ligation reaction. We have emphasized the role of metal ions in the reaction mechanism because mechanistic studies have demonstrated that the RNA phosphodiester chemistry catalyzed by all known ribozymes and by many protein enzymes depends on divalent metal cations[6−8] and because divalent metal ions are considered to have been important catalysts in the prebiotic chemical environment.[3,9]

† Present address: Whitehead Institute for Biomedical Research, Cambridge, MA 02142.

⊗ Abstract published in *Advance ACS Abstracts,* March 1, 1996.

(1) Orgel, L. E. *J. Theor. Biol.* **1986**, *123*, 127−149.

(2) Joyce, G. F. *Cold Spring Harbor Symp. Quant. Biol.* **1987**, *52*, 41−51.

(3) Joyce, G. F.; Orgel, L. E. In *The RNA World*; Gesteland, R. F., Atkins, J. F., Eds.; Cold Spring Harbor Laboratory Press: Cold Spring Harbor, NY, 1993; pp 1−25.

(4) Bartel, D. P.; Szostak, J. W. *Science* **1993**, *261*, 1411−1418.

(5) Rohatgi, R.; Bartel, D. P.; Szostak, J. W. *J. Am. Chem. Soc.* **1996**, *118*, 0000.

Experimental Section

Reagents. Unlabeled nucleoside triphosphates were purchased from Pharmacia, ribonucleoside phosphoramidites were from ChemGenes, and [γ-^{32}P]ATP and the R_p and S_p isomers of [α-S]GTP were from NEN. T7 RNA polymerase was from USB, T4 polynucleotide kinase was from New England Biolabs, calf intestinal alkaline phosphatase was from Boehringer Mannheim, and RNasin RNase inhibitor was from Promega. Buffers (BES, Tris, CHES, and Bis-Tris propane) were purchased from Sigma. All metal salts were purchased from Aldrich and were of the highest purity available: $MgCl_2$ (99.995%), $MnCl_2$ (99.99%), $CaCl_2$ (99.99+%), $SrCl_2$ (99.995%), $BaCl_2$ (99.999%), $Pb(CH_3CO_2)_2$ (99.999%), $ZnCl_2$ (99.999%), $CuCl_2$ (99.9%), KCl (99.98%), and KOAc (99+%).

RNA Synthesis and Purification. The 13-nt template RNA (5′-GAGAACCGACUGG-3′) was chemically synthesized using ribonucleoside phosphoramidites on a Millipore Expedite nucleic acid synthesizer. The synthetic RNA was deprotected using 3:1 aqueous NH_4OH/CH_3CH_2OH for 12 h at 55 °C. The supernatant was removed, passed through a 0.2 μm filter to remove CPG particles, and dried under vacuum. The resulting solid was resuspended with sonication in 700 μL of 1 M tetrabutylammonium fluoride (TBAF) in THF (Aldrich). After incubation for 2−3 days at room temperature in the dark, 700 μL of a 1:1 H_2O/CH_3CN solution with 150 mM NH_4OAc was added, and the RNA purified by HPLC on a preparative scale anion exchange column (Dionex NucleoPac), using aqueous ammonium acetate/10% acetonitrile as the eluent.

The 10-nt primer RNA and the 7-nt ligator RNA (Figure 1) were prepared by run-off transcription from synthetic DNA oligonucleotides,[10] purified on 20% polyacrylamide/8 M urea gels (1.2 mm thick, 40 cm long), and eluted from the gels by the crush and soak method in 0.3 M NaOAc. (Ligation rates did not change when chemically synthesized primer was substituted for enzymatically synthesized primer.) Chemically synthesized primer was 5′-end-labeled using T4 polynucleotide kinase and 100 μCi of [γ-^{32}P]ATP. Enzymatically synthesized primer was dephosphorylated with calf alkaline phosphatase and purified on 20% polyacrylamide/8 M urea gel prior to 5′-end-labeling. The 5′-end-labeled primers were phenol extracted three times, chloroform extracted, and ethanol precipitated.
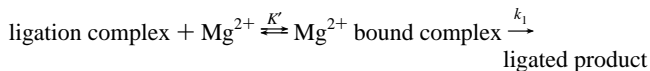
To facilitate synthesis of GDP- and [α-S]GTP-substituted ligator RNAs, the ligator sequence was redesigned to have a unique guanosine residue at the 5′ end (5′-GCUCCU-3′), and the template was concurrently changed (5′-AGGAGCGACUGG-3′). These changes did not alter the base pairs immediately flanking the ligation junction. The GDP- and [α-S]GTP-substituted ligators were synthesized enzymatically by replacing GTP with either GDP or [α-S]GTP in the transcription reactions.

Ligation Reaction. Reactions were performed in 10 μL volumes with 0.4 μM 5′-end-labeled primer, 2.5 μM template, 3 μM ligator, 200 mM KCl, 50 mM buffer at the indicated pH, and the indicated divalent cation. The buffers used were BES (pH 6.4−7.8), Tris (pH 7.3−8.8), CHES (pH 8.6−10.0), and Bis-Tris propane (pH 6.3−9.5). All pH values given have been adjusted for the temperature and other reaction components. Unless otherwise noted, all reactions were incubated at 37 °C in a circulating air incubator for time periods ranging from 12 to 100 h. All metals except Pb^{2+} were used as their chloride salts; since $PbCl_2$ is insoluble, these reactions were performed with $Pb(OAc)_2$; KOAc also replaced KCl. Substitution of KOAc for KCl did not affect ligation rates with any of the divalent cations. At each pH value, the rates were measured using at least two different buffers and did not significantly change with the identity of the buffer.

All reactions were stopped by adding an equal volume of 200 mM EDTA, 8 M urea, 0.02% xylene cyanol, and 0.05% bromphenol blue, followed by freezing at −80 °C. Reaction products were separated from reactants on 20% polyacrylamide/8 M urea gels (0.4 mm thick

and 40 cm long). Radioactivity was quantitated using a Molecular Dynamics PhosphorImager.

Kinetic Analysis. In the time ranges examined ($\leq$100 h), the fraction of labeled primer converted to product was a linear function of time. Since oligonucleotide ligation is a pseudo-first-order process, the slope of such a plot is equal to k_{obs}, the pseudo-first-order rate constant. The hyperbolic saturation curves obtained from Mg^{2+} concentration courses were fit to Michaelis−Menten type equations that assume a single Mg^{2+} binding site. The following kinetic scheme was used:

$$\text{ligation complex} + Mg^{2+} \underset{}{\overset{K'}{\rightleftharpoons}} Mg^{2+} \text{ bound complex} \xrightarrow{k_1} \text{ligated product}$$

The ligation complex is the ligator−primer−template double helical complex (Figure 1). Since k_1 is almost certainly very slow in comparison to the rate of breakdown of the Mg^{2+} bound complex, Mg^{2+} binding can be assumed to be at equilibrium, with K' as the equilibrium constant. Michaelis−Menten type analysis[11] leads to the following equation:

$$k_{obs} = \frac{\text{ligation rate}}{[\text{ligation complex}]_o} = \frac{k_1[Mg^{2+}]}{K' + [Mg^{2+}]} \quad (1)$$

In the text, $[Mg^{2+}]_{1/2}$ (the Mg^{2+} concentration at which k_{obs} is half-maximal) refers to K'.

Temperature Dependence of the Ligation Rate. Reactions were performed beneath a mineral oil overlay in 10 μL volumes containing 0.4 μM 5′-end-labeled primer, 2.5 μM template, 3 μM ligator, 200 mM KCl, 100 mM Mg^{2+}, and 50 mM CHES, pH 8.9. The buffer pH was adjusted to account for the effect of temperature on pH. Each rate was determined at least twice in independent experiments and averaged; k_1 values were derived using eq 1 shown above. The Eyring equation used for the determination of activation parameters is as follows:[12]

$$k_1 = [k_b T/h] \exp[-\Delta H^{\ddagger}/(RT)] \exp[\Delta S^{\ddagger}/R] \quad (2)$$

k_b is the Boltzmann constant, h is the Planck constant, R is the universal gas constant, and T is the absolute temperature.

Data Analysis. The data were analyzed using KaleidaGraph (Abelbeck Software). Due to the low rate of the reaction, long incubation times (up to 100 h) were required, and the variability between data obtained from experiments set up on different days using different reaction mixes was considerable (usually ranging from −50% to +100%). Reactions set up on the same day with the same reaction mixes were more reproducible (±20%). All error values are standard error values based on the nonlinear least-squares fit of the observed data to theoretical equations.

Results

Effects of pH and Divalent Metal Cations. We examined a template-directed oligonucleotide ligation in which a 13-nt template RNA aligns, by contiguous Watson−Crick base-pairing, a 10-nt primer RNA in juxtaposition with a 7-nt ligator RNA (Figure 1). The 3′-hydroxyl of the primer attacks the 5′-triphosphate of the ligator to generate the 17-nt ligation product, with release of pyrophosphate. All reactions included 5′-end-labeled primer at a concentration of 0.4 μM, and sufficient template and ligator (2.5 and 3 μM, respectively) to ensure that essentially all of the primer was in a primer−template−ligator complex. Increasing the template and ligator concentrations to 30 and 50 μM, respectively, had no effect on the rate at temperatures ranging from 0 to 37 °C, pH values ranging from 6.5 to 9.0, and Mg^{2+} concentrations ranging from 10 to 600

(6) Pan, T.; Long, D. M.; Uhlenbeck, O. C. In *The RNA World*; Gesteland, R. F., Atkins, J. F., Eds.; Cold Spring Harbor Laboratory Press: Cold Spring Harbor, NY, 1993; pp 271−302.

(7) Pyle, A. M. *Science* **1993**, *261*, 709−714.

(8) Yarus, M. *FASEB J.* **1993**, *7*, 31−39.

(9) Joyce, G. F. *Nature* **1989**, *338*, 217−224.

(10) Milligan, J. F.; Groebe, D. R.; Witherell, G. W.; Uhlenbeck, O. C. *Nucleic Acids Res.* **1987**, *15*, 8783−8798.

(11) Fersht, A. *Enzyme Structure and Mechanism*; W.H. Freeman and Co.: New York, 1985.

(12) Lowry, T. H.; Richardson, K. S. *Mechanism and Theory in Organic Chemistry*, 3rd ed.; HarperCollins Publishers: New York, 1987; pp 202−211.
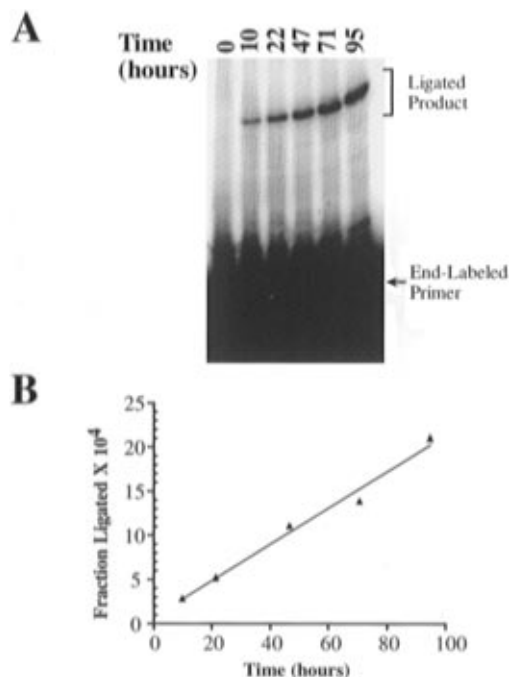
Figure 2. Representative time course of the ligation reaction. (A) An autoradiogram of a denaturing 20% polyacrylamide gel used to separate labeled primer from the ligation product. The gel shows a time course of the ligation reaction performed in 100 mM Mg^{2+} at pH 9.0. (B) The fraction of primer converted to product is a linear function of time in the time ranges used throughout this study. The slope of this plot (k_{obs}) is 2.1×10^{-5} h^{-1}.
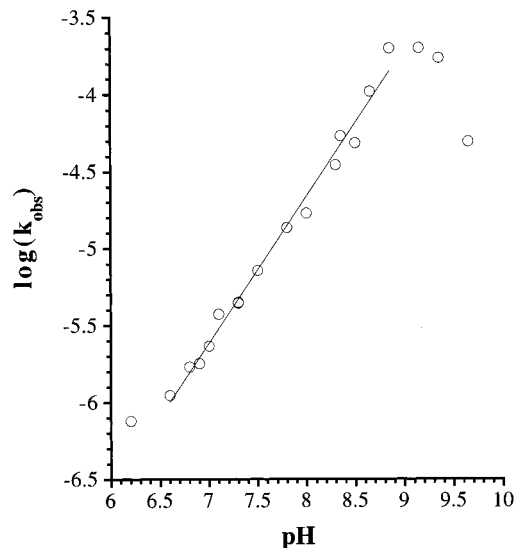

Figure 3. pH dependence of k_{obs}. The slope of the best-fit line to data points between pH 6.5 and pH 9.0 is 0.95. Reactions were performed at 37 °C using 100 mM Mg^{2+} and BES, Tris, or CHES buffer.

mM (data not shown). This confirmed that the template and ligator concentrations used throughout this study were sufficiently above the K_d of the primer−ligator−template complex to yield a pseudo-first-order process. A representative time course of the oligonucleotide ligation reaction is shown in Figure 2.

The ligation rate was measured as a function of pH (Figure 3). A plot of the logarithm of k_{obs} against pH is linear, with a slope of 1.0, between pH 6.5 and 9.0. The ligation rate did not vary with changes in buffer concentration or with the identity of the buffer. Above pH 9.2, ligation rates were slower than predicted from extrapolation of rates at lower pH values (Figure 3). This leveling off is probably a result of the disruption of
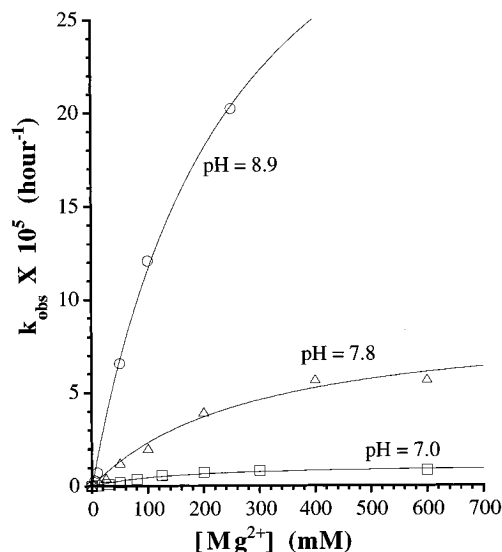

Figure 4. k_{obs} as a function of Mg^{2+} concentration at pH 7.0 (squares), pH 7.8 (triangles), and pH 8.9 (circles). The lines shown are the nonlinear least-squares fits of Michaelis−Menten curves to the data. Extracted values for k_1 and $[Mg^{2+}]_{1/2}$ are as follows: pH 7.0, $k_1 = (1.1 \pm 0.1) \times 10^{-5}$ h^{-1}, $[Mg^{2+}]_{1/2} = 150 \pm 40$ mM; pH 7.8, $k_1 = (9.0 \pm 1.0) \times 10^{-5}$ h^{-1}, $[Mg^{2+}]_{1/2} = 284 \pm 74$ mM; pH 8.9, $k_1 = (4.1 \pm 0.5) \times 10^{-4}$ h^{-1}, $[Mg^{2+}]_{1/2} = 253 \pm 48$ mM.

the double helix resulting from the deprotonation of guanosine (N^1, $pK_a = 9.4$) and uridine (N^3, $pK_a = 9.4$) residues.[13] Above pH 9.2, the rate of nonspecific degradation also sharply increased (data not shown). This is consistent with the disruption of the double helix because single-stranded RNA is much more susceptible to base hydrolysis than is double-stranded RNA.[5,13,14] A similar plateauing of cleavage rate at pH ≥ 9.0 is observed with the hammerhead ribozyme and has also been attributed to the disruption of base-pairing.[15] The pH−rate profile shown in Figure 3 was performed at subsaturating Mg^{2+} concentrations (100 mM) because rates could not be reliably measured at saturating concentrations. At these higher concentrations, nonspecific RNA hydrolysis becomes particularly severe and limits reproducibility.[15−17]

Plots of k_{obs} against the Mg^{2+} concentration (Figure 4) are consistent with a single, saturable Mg^{2+} binding site[4] (but see below for further discussion of this point). Ligation was undetectable in the absence of Mg^{2+} even though the reactions contained 200 mM KCl to stabilize the RNA double helix. Addition of 10 mM spermidine did not alleviate the Mg^{2+} requirement. At 100 mM Mg^{2+}, the omission of KCl had no effect on the ligation rate (data not shown). The effects of pH and Mg^{2+} seem to be independent; at three different pH values, the $[Mg^{2+}]_{1/2}$ values are in the same range (150−280 mM) (Figure 4).

We then examined a series of divalent metal cations for their ability to substitute for Mg^{2+}. Mn^{2+}, Ca^{2+}, Ba^{2+}, and Sr^{2+} could promote ligation in the absence of Mg^{2+} (Figure 5). However, Pb^{2+}, Zn^{2+}, and Cu^{2+} were not active in the concentration and pH ranges tested. Ligation was also not catalyzed by either the $[UO_2]^{2+}$ ion (1−10 mM, pH 7.0) or Montmorillonite clay

(13) Saenger, W. *Principles of Nucleic Acid Structure*; Springer-Verlag: New York, 1984; pp 201−219.
(14) Farkas, W. R. *Biochim. Biophys. Acta.* **1968**, *155*, 401−409.
(15) Dahm, S. C.; Derrick, W. B.; Uhlenbeck, O. C. *Biochemistry* **1993**, *32*, 13040−13045.
(16) Butzow, J. J.; Eichorn, G. L. *Biopolymers* **1965**, *3*, 95−107.
(17) Behlen, L. S.; Sampson, J. R.; DiRenzo, A. B.; Uhlenbeck, O. C. *Biochemistry* **1990**, *29*, 2515−2523.
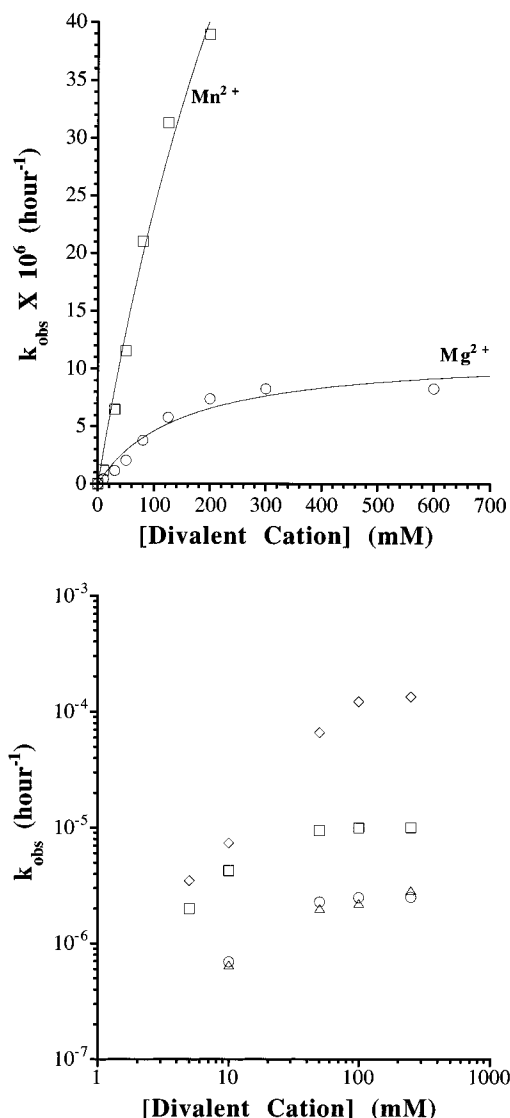
Figure 5. Effects of substituting Mg^{2+} with a series of divalent cations. (A, top) Change in k_{obs} as a function of Mg^{2+} (circles) and Mn^{2+} (squares) concentrations at pH 7.0. The values of k_1 for the Mg^{2+} and Mn^{2+} reactions are $(1.1 \pm 0.1) \times 10^{-5}$ h^{-1} and $(1.2 \pm 0.4) \times 10^{-4}$ h^{-1}, respectively. (B, bottom) Change in k_{obs} as a function of Mg^{2+} (diamonds), Ca^{2+} (squares), Sr^{2+} (triangles), and Ba^{2+} (circles) concentrations at pH 8.7.

(50 mg/mL, pH 7.0), both of which effectively promote the polymerization of adenosine 5'-phosphorimidazolides.[18,19]

A variety of factors limited the pH and concentration ranges under which reproducible data on the catalytic efficiency of these metal ions could be obtained. Pb^{2+} and the transition metal ions promote the rapid degradation of RNA at pH values above 7.5.[6,14,16] Under our reaction conditions, relatively low concentrations ($\sim$20 mM) of Pb^{2+}, Fe^{2+}, Cu^{2+}, and Mn^{2+} almost completely degraded the RNA at pH values above 7.8 (data not shown). These ions also form insoluble hydroxides much more readily than the alkaline earth metals at pH values above 7.0, potentially reducing the free metal ion concentration as well as precipitating the RNA.[15,17,20,21] Finally, the transition metal

(18) Shimazu, M.; Shinozuka, K.; Sawai, H. *Angew. Chem., Int. Ed. Engl.* **1993**, *32*, 870−872.

(19) Ferris, J. P.; Ertzem, G. *Science* **1992**, *257*, 1387−1389.

(20) Kragten, J. *Atlas of Metal-Ligand Equilibria in Aqueous Solution*; Halsted Press: Chichester, England, 1978.

(21) Westermann, K.; Naser, K. H.; Brandes, G. *Inorganic Chemistry*, 12th ed.; VEB Deutscher Verlag fur Grundstoffindustrie: Leipzig, Germany, 1986; pp 53-55.

ions readily react with dissolved oxygen at higher pH values to form metal oxides.[15,20,21] Because of these limitations, Mn^{2+} and Pb^{2+} were used only at pH values below 7.5, and Zn^{2+} below pH 8.3. In addition, we were only able to use Pb^{2+} at concentrations of $\leq$15 mM, Zn^{2+} at $\leq$50 mM, and Mn^{2+} at $\leq$200 mM.

At pH 7.0, the Mn^{2+}-catalyzed rate was 5−7 times faster than the rate at the equivalent concentration of Mg^{2+} (Figure 5A). Although the rate at saturating metal ion concentrations could not be measured directly, curves fitted to the data suggest that the rate at saturating Mn^{2+} concentrations (k_1) is $\sim$10-fold higher than the rate at saturating Mg^{2+} concentrations. The catalytic efficiency of Mg^{2+} was compared to that of Ca^{2+}, Sr^{2+}, and Ba^{2+} at pH 8.7 (Figure 5B). At a concentration of 250 mM, which appears to be close to saturation for all four metal ions, the Mg^{2+}-catalyzed rate was $\sim$8−13 times faster than the Ca^{2+}-catalyzed rate and $\sim$45−50 times faster than the Ba^{2+}- and Sr^{2+}-catalyzed rates. The catalytic efficiencies of these divalent cations can therefore be ordered as follows: $Mn^{2+} > Mg^{2+} > Ca^{2+} > Ba^{2+} = Sr^{2+}$.

Pb^{2+} and Zn^{2+} were added to the ligation reaction in the presence of Mg^{2+}. Whereas Zn^{2+} markedly inhibited the reaction (Figure 6A), Pb^{2+} was an extremely efficient cocatalyst (Figure 6B). When 10 mM Pb^{2+} was included, the ligation rate at pH 7.3 was $\sim$65-fold faster than the rate with 100 mM Mg^{2+} alone. In the presence of Pb^{2+}, the reaction still displayed saturation kinetics for Mg^{2+}; however, the $[Mg^{2+}]_{1/2}$ for the reaction was reduced from $\sim$250 to $\sim$20 mM (Figure 6C). k_1 was also increased in the presence of Pb^{2+}, and this effect could not be competed away by Mg^{2+} concentrations as high as 300 mM.

Activation Parameters for Oligonucleotide Condensation. A Michaelis−Menten type kinetic scheme was proposed to describe diphosphate-activated oligonucleotide condensation (see the Experimental Section). The temperature dependence of k_1 was determined, and the Eyring equation was used to determine activation parameters for oligonucleotide ligation, with the assumption that k_1 is a true microscopic rate constant.[12] An Eyring plot (Figure 7) is linear in the range of 0−37 °C and yields a $\Delta H^{\ddagger}$ value equal to 16.5 ± 0.7 kcal/mol [69 ± 3 kJ/mol] and a $\Delta S^{\ddagger}$ value equal to -19.5 ± 2.5 eu [82 ± 10 J mol^{-1} K^{-1}] for oligonucleotide ligation.

Substitutions at the Attacking Nucleophile and the Leaving Group. We determined the effect of alterations of the attacking nucleophile and leaving group on the reaction rate. Pyrophosphate should be a much better leaving group than phosphate because the fourth (and last) pK_a of pyrophosphate (9.1) is almost 3 units below the third (and last) pK_a of phosphate (12.0).[22] This difference may be enhanced in the presence of metal ions with the potential to complex with the β- and γ-phosphates, and thus activate the leaving group. We could not detect ligation when a monophosphate-activated ligator (i.e., an oligonucleotide beginning with a 5'-diphosphate) replaced a diphosphate-activated ligator (i.e., an oligonucleotide beginning with a 5'-triphosphate), indicating that monophosphate-activated ligation is at least 90 times slower than diphosphate-activated ligation (data not shown).

To determine the sensitivity of the reaction to the strength of the attacking nucleophile, the primer was chemically synthesized with 2'-deoxycytosine in place of cytosine at the 3' end. The pK_a of the 3'-hydroxyl in cytosine (p$K_a = 12.5$) is over 3 units lower than the pK_a of the 3'-hydroxyl in deoxy-

(22) Dawson, R. M. C.; Elliott, D. C.; Elliott, W. H.; Jones, K. M. *Data for Biochemical Research*; Clarendon Press: Oxford, 1986; pp 400−412.

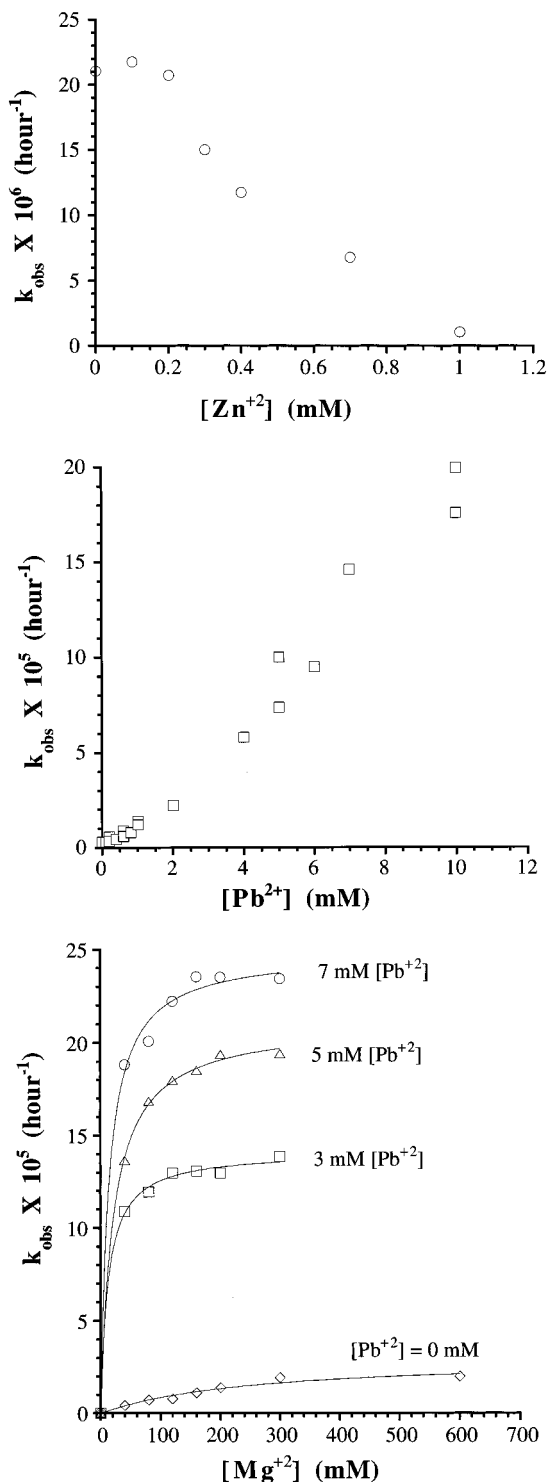**Figure 6.** Effects of Zn^{2+} and Pb^{2+} when added to the ligation reaction in the presence of Mg^{2+}. (A, top) k_{obs} as a function of Zn^{2+} concentration in the presence of 100 mM Mg^{2+}, pH 7.9. (B, middle) k_{obs} as a function of Pb^{2+} concentration in the presence of 100 mM Mg^{2+}, pH 7.3. (C, bottom) k_{obs} as a function of Mg^{2+} concentration (at pH 7.4) in the presence of 0 mM (diamonds), 3 mM (squares), 5 mM (triangles), and 7 mM (circles) Pb^{2+}. Values of k_1 and $[Mg^{2+}]_{1/2}$ were obtained from best-fit curves (0 mM Pb^{2+}, $k_1 = (3.1 \pm 0.4) \times 10^{-5}$ h^{-1}, $[Mg^{2+}]_{1/2} = 260 \pm 70$ mM; 3 mM Pb^{2+}, $k_1 = (1.4 \pm 0.02) \times 10^{-4}$ h^{-1}, $[Mg^{2+}]_{1/2} = 12 \pm 2$ mM; 5 mM Pb^{2+}, $k_1 = (2.1 \pm 0.02) \times 10^{-4}$ h^{-1}, $[Mg^{2+}]_{1/2} = 21 \pm 1$ mM; 7 mM Pb^{2+}, $k_1 = (2.5 \pm 0.05) \times 10^{-4}$ hour^{-1}, $[Mg^{2+}]_{1/2} = 14 \pm 3$ mM).

cytosine ($pK_a > 15.7$).[23,24] This reduction is attributed to the electron-withdrawing (or inductive) effect of the 2′-hydroxyl and its ability to form an intramolecular hydrogen bond with
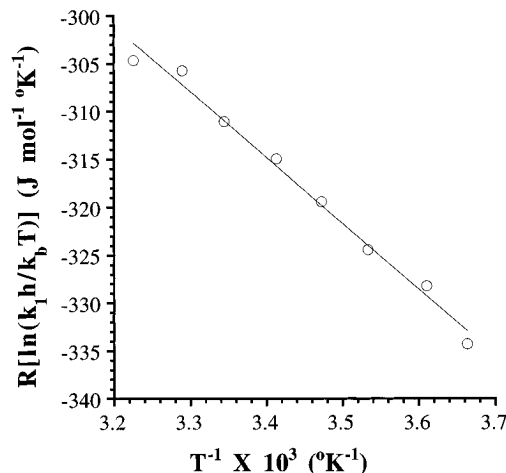

Figure 7. Eyring plot for the assumed one-step conversion of the Mg^{2+}-bound ligation complex to ligated product. Activation parameters are $\Delta H^\ddagger = 69 \pm 3$ kJ/mol and $\Delta S^\ddagger = -19.5 \pm 2.5$ eu. The deviation from linearity seen at 45 °C indicates that the ligator−template−primer complex is starting to melt at temperatures above 37 °C, leading to a decline in rate.

the 3′-oxygen. At pH 9.0 and 100 mM Mg^{2+}, the ligation rate with the 2′-deoxycytosine primer was 16-fold lower than the rate with the control cytosine primer (data not shown).

Substitution of an oxygen by sulfur is a commonly used technique for probing the mechanism of phosphoryl transfer reactions.[25−27] In order to study the effects of thio substitution on oligonucleotide condensation, we enzymatically synthesized two ligator RNAs that had either the S_p or the R_p isomer of guanosine 5′-thiotriphosphate ([α-S]GTP) at the 5′-end. The pH−rate profiles of the R_p and S_p thio-substituted ligators at 100 mM Mg^{2+} are markedly different from the pH−rate profile of the control (unsubstituted) ligator (Figure 8). In contrast to the unsubstituted ligator, the ligation rate was relatively insensitive to pH for both the S_p and the R_p thio-substituted ligators. As a result, at pH 6.6, the thio-substituted ligators reacted 10 times faster than the control ligator, while at pH 9.0, the control ligator reacted 12 times faster. This difference is not dependent upon the identity of the buffer or the time of incubation (data not shown). The addition of dithiothreitol also had no effect on these pH−rate profiles. The lower ligation rate observed at pH 8.9 using the thio-substituted ligators is not due to the differential degradation of the ligation products.

Discussion

We have studied the mechanism of nonenzymatic, template-directed oligoribonucleotide ligation. This reaction involves the nucleophilic attack of the 3′-hydroxyl of one oligonucleotide on the α-phosphate of the 5′-triphosphate of an adjacent oligonucleotide, with displacement of pyrophosphate and formation of a 3′−5′ phosphodiester bond linking the two oligonucleotides. The chemistry of this reaction is identical to that catalyzed by the DNA and RNA polymerases found in all living organisms, and by certain ribozymes recently isolated from random sequences by in vitro selection. While the enzymatic reactions have been the subject of intense study, the non-enzymatic reaction has not previously been characterized;

(23) Izatt, R. M.; Hansen, L. D.; Rytting, J. H.; Christensen, J. J. *J. Am. Chem. Soc.* **1965**, *87*, 2760−2761.
(24) Birnbaum, G. I.; Giziewicz, J.; Huber, C. P.; Shugar, D. *J. Am. Chem. Soc.* **1976**, *98*, 4640−4644.
(25) Knowles, J. R. *Annu. Rev. Biochem.* **1980**, *49*, 877−919.
(26) Frey, P. A. *Tetrahedron* **1982**, *38*, 1541−1567.
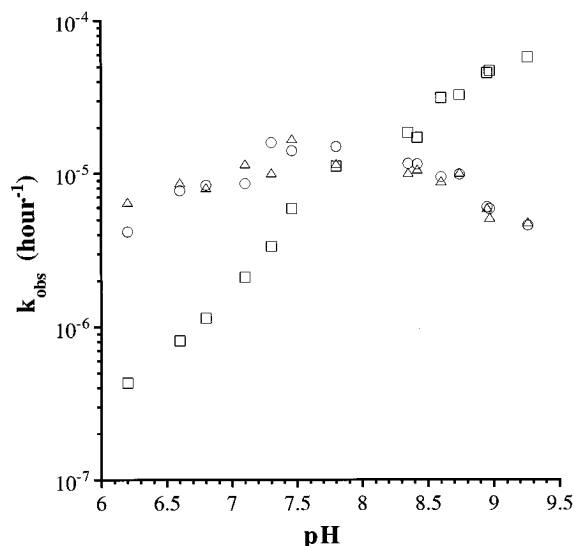(27) Eckstein, F. *Annu. Rev. Biochem.* **1985**, *54*, 367−402.

Template-Directed Oligoribonucleotide Ligation

J. Am. Chem. Soc., Vol. 118, No. 14, 1996 3337

Figure 8. k_{obs} as a function of pH for the S_p α-thio-substituted ligator (triangles), the R_p α-thio-substituted ligator (circles), and the unsubstituted control ligator (squares). Reactions were performed under standard conditions with 100 mM Mg^{2+}. The plot for the control ligator has a slope of 0.8.

a greater understanding of the nonenzymatic reaction is necessary to achieve a full understanding of the ways that protein enzymes and ribozymes accelerate this reaction.

The nonenzymatic reaction is catalyzed by divalent metal ions. Plots of k_{obs} against Mg^{2+} concentration (Figure 4) suggest a Mg^{2+} binding site with half-maximal activity at 150–300 mM. However, nucleoside triphosphates are well known to chelate divalent metal ions quite tightly; for example, ATP^{4-} binds Mg^{2+} with a dissociation constant of 10–100 μM.[22] Since our reaction conditions include much higher concentrations of Mg^{2+}, it is likely that the oligonucleotide triphosphate is tightly complexed with one Mg^{2+}, and that the observed dependence of the ligation reaction on high concentrations of Mg^{2+} reflects a second weak Mg^{2+} binding site. The precise locations of the strong and weak binding sites are of great interest. One candidate for the location of the strong site is the β- and γ-phosphates of the 5′-triphosphate of the ligator RNA. In solution, Mg^{2+} is thought to exist as a mixture of bidentate chelates with the α–β-, α–γ-, and β–γ-phosphates of nucleoside triphosphates,[28] although some recent studies are consistent with predominant coordination of Mg^{2+} with the β- and γ-phosphates.[29,30] Coordination of a metal ion to the β- and γ-phosphates could accelerate the reaction by decreasing the pK_a of the pyrophosphate leaving group. Enzymes could accelerate the reaction by stabilizing this form; for instance, DNA and RNA polymerases use the βγ-bidentate chelate form of nucleoside 5′-triphosphates.[31] Although the weak site is necessary for observable ligation, we know very little about it. In fact, although the data are reasonably well fit by a single saturable binding site, the theoretical curves generally overestimate the rates at low metal ion concentrations. This slight sigmoidicity could be due to a requirement for two weakly bound metal ions, or to weaker than expected binding to the triphosphate site. Alternative explanations for apparent satura-

tion such as general ionic effects on duplex geometry, screening effects, or the binding of an inhibitory Mg^{2+} cannot be ruled out.

The pH–rate profile of the reaction suggests a role for the weakly bound metal ion in deprotonation of the attacking hydroxyl. In the presence of Mg^{2+}, a plot of log k_{obs} vs pH is linear, with a slope of 0.95 between pH 6.5 and pH 9.0. Such a plot indicates that some deprotonation step is required to reach the transition state of the reaction.[11,32] In this nonenzymatic reaction, the most likely site for an essential deprotonation is the attacking 3′-hydroxyl. This deprotonation could be facilitated by the weakly bound Mg^{2+} either directly, by coordination to O3′, thus lowering the pK_a of the 3′-hydroxyl, or indirectly, by proton transfer to metal hydroxide ($[M(OH)]^+$). Linear pH–rate profiles have been used to infer such a role of M^{2+} in catalysis by t-RNA^{Phe}, RNase P, hammerhead, and Group I ribozymes.[15,33–35] In the group I intron ribozymes, thio and metal substitution experiments have shown that the catalytic metal is directly coordinated with the attacking 3′-hydroxyl.[33] The nonspecific hydrolysis of RNA catalyzed by divalent metal cations is also thought to involve a metal-bound hydroxide as the active species.[6]

We obtained evidence for a role of the weakly bound divalent metal ion in the deprotonation step of the ligation reaction by varying the identity of the metal ion used for catalysis. A similar analysis has been performed for the hammerhead ribozyme and for the catalysis of nonspecific RNA hydrolysis by divalent metal cations.[6,14,15] As with the hammerhead study our studies were complicated by the fact that ligation rates had to be measured at subsaturating metal ion concentrations. However, Mg^{2+}, Mn^{2+}, Ca^{2+}, Sr^{2+}, and Ba^{2+} bind to the primer–ligator–template complex with approximately similar affinities (Figure 5b), although these apparent saturation curves are subject to the same caveats as noted above for Mg^{2+}. In the absence of idiosyncratic geometrical effects, the ligation rate should inversely correlate with the pK_a of the metal ion (at a fixed pH below the pK_a values of the divalent cations) because the ratio of $[M(OH)]^+$ to $[M(H_2O)]^{2+}$ will decrease as the pK_a increases. In accord with this prediction, we have found that, among the metal ions that catalyze ligation without the addition of Mg^{2+}, activity (Mn^{2+} > Mg^{2+} > Ca^{2+} > Sr^{2+} = Ba^{2+}) correlates inversely with pK_a (Mn^{2+}, 10.6; Mg^{2+}, 11.4; Ca^{2+}, 12.9; Sr^{2+}, 13.3; Ba^{2+}, 13.5). At pH 8.7, the ligation rate with 200 mM Ca^{2+} is ~13-fold lower than that with 200 mM Mg^{2+}. Ca^{2+} and Mg^{2+} have very similar properties,[6,22] but the pK_a of Ca^{2+} is 1.4 units higher than that of Mg^{2+}. Therefore, at a given pH (below the pK_a values of Ca^{2+} and Mg^{2+}), the concentration of $[Ca(OH)]^+$ will be 25 times lower than the concentration of $[Mg(OH)]^+$, a value which correlates well with the 13-fold difference in rates. Similarly, at pH 7.0, the 6–10-fold higher rate seen with Mn^{2+} as compared to Mg^{2+} correlates well with the 6-fold higher concentration of $[Mn(OH)]^+$. Finally, the ~50-fold higher rate seen with Mg^{2+} as compared to Ba^{2+} and Sr^{2+} also agrees well with the 100-fold higher concentration of $[Mg(OH)]^+$. On the basis of these trends, we propose that a metal hydroxide bound near the ligation junction, or a metal directly coordinated to O3′, catalyzes ligation by accelerating deprotonation of the attacking hydroxyl.

In the absence of Mg^{2+}, Pb^{2+} and Zn^{2+} display no catalytic activity even though their pK_a values are much lower than the

(28) Ramirez, F.; Maracek, J. F. *Biochem. Biophys. Acta* **1980**, *589*, 21–29.

(29) Huang, S. L.; Tsai, M.-D. *Biochemistry* **1982**, *21*, 951–959.

(30) Takeuchi, H.; Murata, H.; Harada, I. *J. Am. Chem. Soc.* **1988**, *110*, 392–297.

(31) Kornberg, A.; Baker, T. *DNA Replication*, 2nd ed.; W.H. Freeman and Co.: New York, 1992; pp 135–136.

(32) Herschlag, D.; Eckstein, F.; Cech, T. R. *Biochemistry* **1993**, *32*, 8312–8321.

(33) Piccirilli, J. A.; Vyle, J. S.; Caruthers, M. H.; Cech, T. R. *Nature* **1993**, *361*, 85–87.

(34) Smith, D.; Pace, N. R. *Biochemistry* **1993**, *32*, 5273–81.

(35) Brown, R.; Dewan, J.; Klug, A. *Biochemistry* **1985**, *24*, 4785–4801.

pK_a values of any of the other ions tested (Pb^{2+}, 7.7; Zn^{2+}, 9.0). Because all reactions include 200 mM KCl, it is unlikely that this reflects dissociation of the RNA duplex. However, in the presence of 100 mM Mg^{2+}, Pb^{2+} is an efficient cocatalyst. The rate acceleration provided by Pb^{2+} in the presence of Mg^{2+} could be due to either Pb^{2+} displacing Mg^{2+} from the weak [M(OH)]$^+$ or M^{2+} binding site or binding to a different catalytic site. The observation that the addition of Pb^{2+} both increases k_1 and decreases [Mg^{2+}]$_{1/2}$ supports the idea that there are two metal binding sites. The fact that Pb^{2+} catalysis depends on the presence of Mg^{2+} can be explained if the strong site must be occupied by Mg^{2+} for ligation to proceed. The 10-fold difference in [Mg^{2+}]$_{1/2}$ for the reaction in the presence and absence of Pb^{2+} may reflect the fact that different sites are being titrated by Mg^{2+} in each case. The high apparent [Mg^{2+}]$_{1/2}$ for the strong site (10−20 mM, compared with the expected 10−100 μM for binding of Mg^{2+} to a triphosphate) could be due to competition with Pb^{2+}. Such competition could also explain the nonlinearity of the k_{obs} vs Pb^{2+} curve (Figure 6B).

In contrast to Pb^{2+}, Zn^{2+} inhibits the reaction in the presence of Mg^{2+}. Zn^{2+} has a low pK_a (9.0) and would be predicted to be an efficient catalyst if it bound to the appropriate site. One possibility is that Zn^{2+} distorts the helix near the ligation junction in such a way that the relative orientation of the acceptor and donor groups is unfavorably altered. Soft transition metals like Zn^{2+} have a greater propensity than Mg^{2+} to complex with base nitrogens, especially N^7, a property which causes them to distort double helices.[13] Zn^{2+}-induced helical distortion may explain why Zn^{2+} alters the regioselectivity of the poly(C) directed polymerization of guanosine 5′-phosphorimidazolide and inhibits the poly(U) directed polymerization of adenosine 5′-phosphorimidazolide.[36]

The relative activities of Mn^{2+}, Mg^{2+}, Ca^{2+}, Sr^{2+}, and Ba^{2+} follow the same order for hammerhead cleavage as for non-enzymatic ligation, suggesting that a metal hydroxide or directly coordinated metal ion may be involved in both cases. The surprising similarities between a cleavage reaction catalyzed by a ribozyme with a complex tertiary structure and a simple nonenzymatic ligation reaction occurring in the context of a helix highlight the possibility that the earliest ribozymes evolved to catalyze reactions by stabilizing the binding of divalent cations in a favorable geometry [8] without changing the underlying reaction mechanism.

The oligonucleotide ligation reaction is similar in many respects to the hydrolysis of phosphodiesters, with the nucleophile being a (presumably) deprotonated 3′-hydroxyl instead of hydroxide ion, and the relevant phosphate being a monoester−monoanhydride instead of a diester. Studies in which the pK_a of the nucleophile and leaving group have been varied, along with thio substitution and isotope effects, have clearly established the associative nature of the transition state for phosphotriester hydrolysis, the dissociative nature of the transition state for phosphomonoester hydrolysis, and the intermediate nature of the transition state for phosphodiester hydrolysis.[37] Several observations in this paper are consistent with an associative transition state, in which there is significant participation of both the nucleophile and the leaving group, for the oligonucleotide ligation reaction.

The activation parameters derived for oligonucleotide condensation can be compared to values which have been derived for other phosphoester transfer reactions. $\Delta S^{\ddagger}$ values for the hydrolysis of phosphomonoesters are small, consistent with a
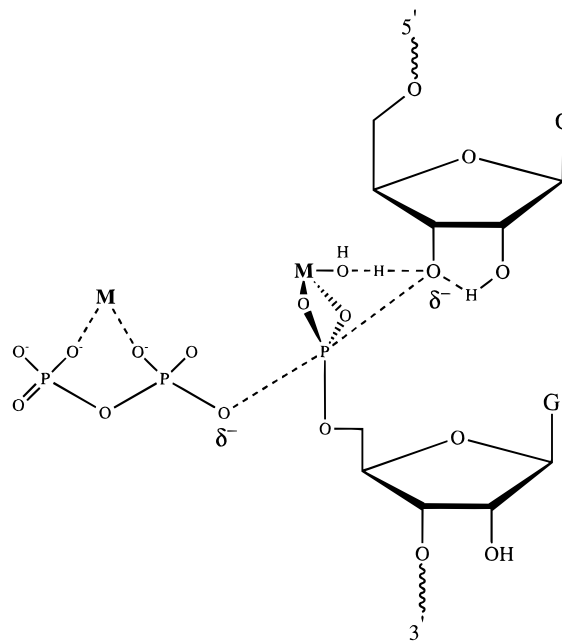

Figure 9. A possible transition state for template-directed oligonucleotide ligation. **M** denotes a divalent metal cation. No evidence has been provided for the coordination of **M** to the α-phosphate.

dissociative, metaphosphate-like transition state.[25,38−40] The $\Delta S^{\ddagger}$ values for phosphodiester and triester hydrolyses are larger[25,38,39] and are considered to be indications of a bimolecular, associative transition state in which there is participation of a specific water molecule. When compared to these values, the $\Delta S^{\ddagger}$ value for oligonucleotide condensation ($\sim$−20 eu) is consistent with an associative transition state. However, the template−primer−ligator oligonucleotide complex is much more complex than the simple substrates used in the hydrolytic studies, and the large value of $\Delta S^{\ddagger}$ could reflect conformational rearrangements that must occur to reach the transition state.

Further suggestive evidence for an associative transition state has been obtained by varying the attacking and leaving groups. The fact that the rate of the reaction decreases greatly when the leaving group is changed from a diphosphate to a monophosphate suggests that the bond between the leaving group and the α-phosphate is significantly weakened in the rate-determining transition state. The reduction in rate caused by substitution of 2′-deoxycytosine for rC at the 3′ end of the primer also suggests that there is nucleophilic participation in the transition state. However, the establishment of rigorous structure−reactivity correlations requires that a series of graded changes be made in the pK_a of the attacking nucleophile and the leaving group, and isolated substitutions can be misleading because of unrelated effects, such as alterations of the metal binding site or steric changes at the ligation junction.[13]

The dramatic change in the pH−rate profile observed with the thio substitution suggests that the reaction mechanism changes upon thio-substitution. In the case of phosphoester transfer reactions, thio substitutions stabilize dissociative transition states and destabilize associative ones.[38,41] For phosphotriesters, thio substitution slows the rate of hydrolysis by a factor of $\sim$10−160 presumably because oxygen is better able to

(36) Bridson, P. K.; Orgel, L. E. *J. Mol. Biol.* **1980**, *144*, 567−577.

(37) Herschlag, D.; Piccirilli, J. A.; Cech, T. R. *Biochemistry* **1991**, *30*, 4844−4854.

(38) Benkovic, S. J.; Schray, K. J. In *The Enzymes*; Boyer, P., Ed.; Academic Press: New York, 1971; Vol. 8, pp 201−208.

(39) Herschlag, D.; Jencks, W. P. *J. Am. Chem. Soc.* **1989**, *111*, 7579−7586.

(40) Kirby, A. J.; Varvoglis, A. G. *J. Am. Chem. Soc.* **1967**, *89*, 415−423.

(41) Herschlag, D.; Jencks, W. P. *J. Am. Chem. Soc.* **1989**, *111*, 7587−7596.

stabilize the increased electron density in the associative transition state.[37] In contrast, thio substitution accelerates reactions of phosphomonoester dianions, which proceed via electron deficient, dissociative transition states that are stabilized by charge donation from the phosphoryl substituents.[37] Thio substitution may increase the dissociative character of the transition state of the ligation reaction to such an extent that the nucleophilicity of the 3′-hydroxyl has little effect on reaction rate, consistent with the flat pH−rate profile seen with the thio-substituted ligators. This postulated change in mechanism requires the unsubstituted reaction to have significant associative character.

On the basis of the above data, we propose a possible transition state for this reaction at high pH (≥ 8.5) (Figure 9). The transition state has associative character, with bonding to both the attacking 3′-hydroxyl and the leaving pyrophosphate. A tightly bound metal ion is coordinated to the β- and γ-phosphates, stabilizing the developing negative charge on the leaving group. A metal hydroxide assists in the deprotonation of the 3′-hydroxyl, producing a partial negative charge on the nucleophile in the transition state. This model suggests ways in which protein and RNA enzymes could promote catalysis.

Enzymes can bind metal ions with high affinity and position them precisely;[8,15] the microenvironment of an enzyme active site may also lower the pK_a of the metal-bound water compared to its value in aqueous solution.[42,43] Finally, enzymes could accelerate the reaction by using electrostatic catalysis to stabilize the developing negative charge on the oxygen atom of the leaving pyrophosphate. Protein enzymes may use bidentate electrophiles (such as the guanidinium groups of arginine residues) in order to coordinate the pyrophosphate; however, RNA enzymes, which do not have such positively charged groups at neutral pH, probably depend on divalent metal cations for electrostatic catalysis.

(42) Jones, D. R.; Lindoy, L. F.; Sargeson, A. M. *J. Am. Chem. Soc.* **1983**, *105*, 7327−7336.

(43) Coleman, J. E.; Chlebowski, J. F. *Advances in Inorganic Biochemistry*; Elsevier: Amsterdam, 1979; Vol. 1, pp 1−66.